

Aggregation-Induced Long-Lived Phosphorescence in Nonconjugated Polyurethane Derivatives at 77 K

Nan Jiang,^{†,||} Guang-Fu Li,^{†,||} Bao-Hua Zhang,[#] Dong-Xia Zhu,^{*,†} Zhong-Min Su,^{*,†} and Martin R. Bryce^{*,§}

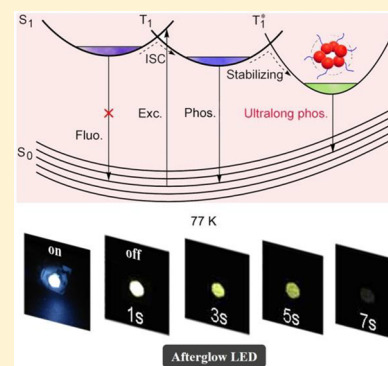
[†]Key Laboratory of Nanobiosensing and Nanobioanalysis at Universities of Jilin Province, Faculty of Chemistry, Northeast Normal University, Renmin Street No. 5268, Changchun 130024, PR China

[#]State Key Laboratory of Polymer Physics and Chemistry, Changchun Institute of Applied Chemistry, Chinese Academy of Sciences, Changchun 130022, PR China

[§]Department of Chemistry, Durham University, Durham DH1 3LE, U.K.

S Supporting Information

ABSTRACT: Achieving long-persistent phosphorescence in polymers is a challenge even at low temperatures. In this work, long-persistent phosphorescence (>1 s) is observed in nonconjugated polyurethane derivatives at 77 K, which is among the longest reported phosphorescent lifetimes for an organic polymer. The mechanism for this unusual behavior has been shown by steady-state photophysical characterization and time-resolved emission spectra to arise from the formation of intra- and/or intermolecular carbonyl clusters at low temperature. The lifetime of long-persistent phosphorescence is increased by the introduction of an aromatic monomer into the nonconjugated polyurethane chains. This is attributed to intra- and/or intermolecular $n-\pi^*$ transitions from electron-rich carbonyl groups to the conjugated aromatic units, thereby enhancing the intersystem crossing rate. Coating an ultraviolet InGaAsN light-emitting diode with a polyurethane derivative as the emitter gives cryogenic afterglow with long-persistent phosphorescence that is observed for up to 7 s with the naked eye.



1. INTRODUCTION

Nonconjugated polymers are emerging as unconventional luminophores that do not possess typical polycyclic π -conjugated chromophoric units, and they have aroused great interest because of their significant academic value and promising technological applications.^{1–5} Compared to the traditional organic luminescent materials, nonconjugated polymers show many advantages in terms of ease of chemical preparation, environmental friendliness, and applications in biological fluorescence imaging, due to their good hydrophilicity, chain flexibility, and structural versatility.⁶ Research in this area is still in its infancy, lacking clear guidelines for polymer design, and the mechanism of luminescence is not well-understood. Generally, the presence of electron-rich heteroatoms, such as nitrogen,^{7–14} oxygen,^{15–19} phosphorus,^{20,21} or sulfur,^{22,23} and/or unsaturated $C=O$,²⁴ $C=C$,²⁵ and $C\equiv N$ ²⁶ subgroups into nonconjugated backbones is necessary for unconventional luminescence. Therefore, it is desirable to develop new types of luminescent nonconjugated polymers and to further probe the mechanism of emission in these systems.

Polyurethanes (PUs) are industrial-scale nonconjugated polymers with many desirable properties, such as facile synthesis, good mechanical toughness, abrasion resistance, and low-temperature resistance. They have found broad applications as shape-memory materials, building insulation,

and components of furniture and fabrics in our daily life.^{27–29} However, their luminescent properties and optoelectronic applications are largely unexplored.^{30–33} We hypothesized that by virtue of the structural flexibility and electron-rich heteroatoms (O and N) nonconjugated polyurethanes could possess interesting photophysical properties due to the following considerations. First, the nonconjugated architecture may effectively avoid aggregation-induced quenching of emission, which is facilitated by strong $\pi-\pi$ stacking interactions in conjugated materials. Consequently efficient emission could occur at high concentrations. Second, the nonconjugated PU structure blocks strong electronic coupling and is therefore favorable for blue emission. Third, because of the good mechanical flexibility of PUs, the individual polymer chains are in close proximity. Excited-state charge-transfer processes may, therefore, readily occur through intermolecular interactions, leading to a small singlet–triplet splitting (ΔE_{ST}) which, in turn, could promote intersystem crossing (ISC) as well as reverse ISC (RISC)³⁴ between singlet (S_1) and triplet (T_1) states, thus prolonging the exciton lifetimes.

In this work, a series of three nonconjugated polyurethanes, PU1–PU3, have been rationally designed: PU1 incorporates

Received: April 5, 2018

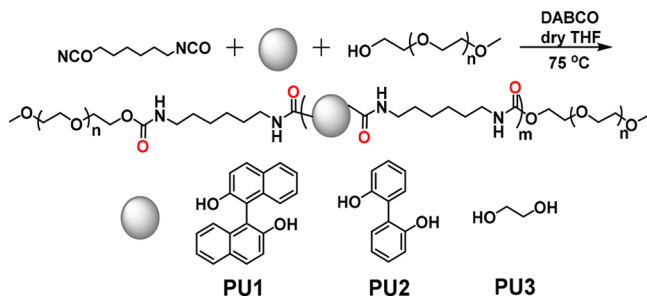
Revised: May 9, 2018

the classical π -aromatic binaphthyl chromophores, whereas PU2 and PU3 have π -aromatic biphenyl chromophores and nonaromatic units, respectively, in the polymer backbones. PU1–PU3 all show unusually long-persistent luminescence (LPL) at 77 K, including PU3 with no aromatic backbone units. There is an increase in luminescent lifetimes with the introduction of aromatic monomer units, indicating that the LPL lifetimes can be rationally tuned by the incorporation of aromatic chromophores into these PU derivatives. Thus, among the three PUs, PU1 exhibits the longest phosphorescent decay times of 1.4 and 0.52 s in solution and powder states, respectively. Steady-state photophysical data and time-resolved emission spectra (TRES) lead to the conclusion that the formation of intra- and/or intermolecular carbonyl clusters at low temperature plays a key role in obtaining long-persistent phosphorescence. These results, therefore, establish that polyurethane derivatives can be designed to display aggregation-induced persistent phosphorescence. Furthermore, benefiting from the excellent LPL at high concentration for PU1, a cryogenic afterglow InGaAsN light-emitting diode (LED) has been fabricated using PU1 as the emitter. Long-persistent phosphorescence is observed for up to 7 s by naked eyes.

2. RESULTS AND DISCUSSION

2.1. Synthesis. The PUs were synthesized by dissolving polyethylene glycol monomethyl ether ($M_w = 200$ g mol⁻¹, 0.396 g, 1.98 mmol) and (R)-1-(2-hydroxynaphthalen-1-yl)naphthalen-2-ol ((R)-BINOL) (2.62 mmol), 2,2'-biphenol (2.62 mmol), or 1,2-ethanediol (2.62 mmol) in anhydrous tetrahydrofuran (THF) (10 mL). Hexamethylene diisocyanate (0.608 g, 3.61 mmol) and 1,4-diazabicyclooctane triethylenediamine (DABCO) (12 mg, 0.06 mmol) were then added to the reaction mixture, which was stirred at 75 °C for 7 h under N₂ until the clear solution became viscous, indicating polymerization had occurred. After the mixture cooled to room temperature, excess diethyl ether was added to precipitate the products PU1 ($M_n = 3118$ g mol⁻¹), PU2 ($M_n = 1845$ g mol⁻¹), and PU3 ($M_n = 3544$ g mol⁻¹), with yields >60% (Scheme 1). The detailed synthetic methods and ¹H NMR and Fourier transform infrared (FTIR) spectroscopic characterization are given in the Experimental Section and Supporting Information.

Scheme 1. Synthetic Routes for PU1, PU2, and PU3



2.2. Physical Properties. Most aggregation-induced emission (AIE) materials are almost nonemissive in both dilute and highly concentrated solutions, whereas bright emission can be observed in the solid and host–guest doped film states because of the restriction of intramolecular motion (RIM).³⁵ At room temperature, PU1–PU3 show faint emission in dilute solution, whereas intense emission is observed in highly

concentrated solution and in the solid states, which is atypical AIE behavior. The absorption spectra of PU1 in different ratios of acetone–water mixtures are depicted in Figure S5a. The major absorption peak at 339 nm is assigned to the R band of an $n \rightarrow \pi^*$ transition, suggesting that O and/or N atoms are conjugated with aromatic rings in the system.³⁶ The progressively enhanced absorption intensity with an extended red edge for increased water % is evidence for the formation of nanoaggregates, which was further established by transmission electron microscopy (TEM) results. The TEM image of PU1 showed dispersed nanoparticles with a diameter in the range of 20–50 nm in dilute acetone solution (1×10^{-5} M) (Figure S6a). However, when the added water fraction reached 90%, irregularly shaped (chains and particles) larger aggregates were formed (Figure S6d). This indicates that nanoaggregation is enhanced by the addition of water which is a poor solvent.

The corresponding emission spectra of PU1 in different ratios of acetone–water mixtures are shown in Figure 1a. PU1

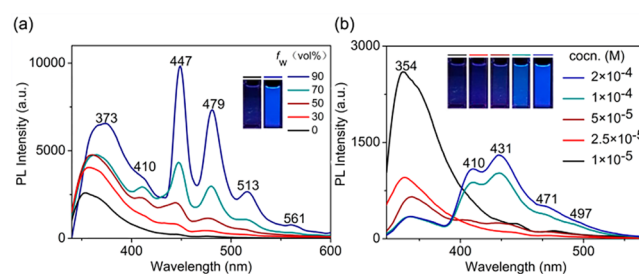


Figure 1. (a) Emission spectra of PU1 (1×10^{-5} M) in acetone–water mixtures with different water fractions (0–90% v/v) at room temperature. Inset: photographs of PU1 ($M_n = 3118$ g mol⁻¹) in pure acetone solution and acetone–water mixture ($f_w = 90\%$) under 365 nm UV illumination. (b) PL spectra of PU1/acetone with different concentrations. Inset: photographs taken under 365 nm UV light.

exhibits faint emission in dilute acetone solution (10^{-5} M), which is considerably increased when the water fraction exceeds ca. 60%. Emission peaks at 373, 410, 447, 479, 513, and 561 nm with different lifetimes (τ) of 1.1, 1.24, 6.32, 6.7, and 6.64 ns are observed. Meanwhile, the emission spectrum of monomer (R)-BINOL was also measured in both the solution and powder states (Figure S7), and only the UV emission with a peak at 370 nm was observed. This indicates that the emission peak at 373 nm in PU1 originates from the excited state of the (R)-BINOL unit. The other emission peaks of PU1 are indicative of the presence of different emissive species in solution, derived from various aggregated structures owing to chain folding and aggregation.²⁶ When the water fraction increases up to 90%, a 100-fold increase in emission intensity of PU1 was observed in comparison with the pure acetone solution. The photoluminescence quantum yield (PLQY) of PU1 is 21%. All the above photophysical results demonstrate that PU1 displays AIE.

In contrast to the typical AIE effect,³⁵ a concentration-dependent emission behavior was observed for PU1 in acetone solution (Figure 1b). The concentrations of PU1 were selected within the range of 1×10^{-5} to 2×10^{-4} M. The emission intensity of PU1 increases when the concentration increased to 1×10^{-4} M and shows emission features similar to those of the acetone/water mixtures at low concentration of 1×10^{-5} M. Meanwhile, the features in the UV–vis absorption spectra of PU1 in acetone (Figure S5b) being similar to the those of

acetone–water mixtures (Figure S5a) demonstrates that the aggregates form in both conditions. TEM reveals that the sizes of nanoparticles increased from ca. 20 nm to ca. 200 nm with an incremental increase in concentration (10^{-5} to 2×10^{-4} M) of PU1 (Figures S6a–c). To investigate the possible influence of hydrogen bonding interactions in the aggregated state, ^1H NMR spectra were recorded for concentrations of 2.5 and 5 mg mL^{-1} of PU1 in $\text{DMSO}-d_6$. The almost identical ^1H NMR spectra for both solutions (Figure S8) with no N–H shift implies that hydrogen bonding interactions are absent or very weak in the aggregated state.³⁷ Thus, it is rational to ascribe the AIE mechanism of PU1 to the formation of carbonyl clusters.^{6,24} As illustrated in Figure 2, the linear PU1 chains

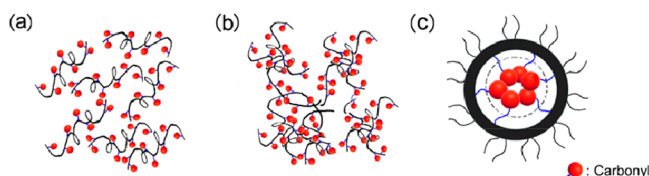


Figure 2. Schematic illustration of PU1 (a) dilute solution, (b) concentrated solution, and (c) carbonyl clusters in the aggregated state.

will be extended in dilute solution, effectively isolating the carbonyl groups and, therefore, leading to only faint emission (Figure 2a). In concentrated solution or the aggregated state, PU1 chains will entangle and approach each other in close proximity to form carbonyl clusters, affording through-space electronic overlap between lone pairs and π electrons (Figure 2b,c). Consequently, in the more rigidified conformations, there is enhanced electronic conjugation, which, in turn, leads to enhanced emission. In previous work, the unconventional emission in nonconjugated linear and hyperbranched polymers, e.g., siloxane-poly(amidoamine) dendrimers, was explained by aggregation of multiple carbonyl groups.^{6,24} LPL of nonconjugated polyacrylonitrile, without any aromatic chromophore in the molecule, has been ascribed to clustering of the pendant cyano groups in concentrated solution and solid samples affording through-space electronic communication.²⁶

The emission spectra of PU1 in the powder state were explored at different excitation wavelengths (Figure S9). Under UV illumination, powder PU1 exhibits bright emission covering the UV and visible regions. The weak lower-energy emission peaks are consistent with those observed in high-concentration acetone solution and acetone/water mixtures (Figure 1a), indicating the presence of various emissive species that might be derived from different carbonyl clusters. The semi-crystallinity of PU1 shown by powder X-ray diffraction (Figure S10) offers additional physical restraints and is favorable for light emission.²⁶

2.3. Cryogenic Long-Persistent Phosphorescence. The photophysical properties of PU1 were further studied at 77 K in dilute 2-methyltetrahydrofuran (2-MeTHF) solution (10^{-5} M). As shown in Figure 3a, upon irradiation with UV light at 365 nm, the steady-state emission spectra showed multiple profiles with major peaks at 409, 437, 463, and 497 nm, which is similar to the behavior at room temperature (Figure 1b). Upon removal of the ultraviolet irradiation, LPL lasting for 2 s with changed emission color was clearly observed by the naked eye (Figure 3a insert images and Supplementary Movie 1). Thus, PU1 exhibits LPL which is rarely observed in a

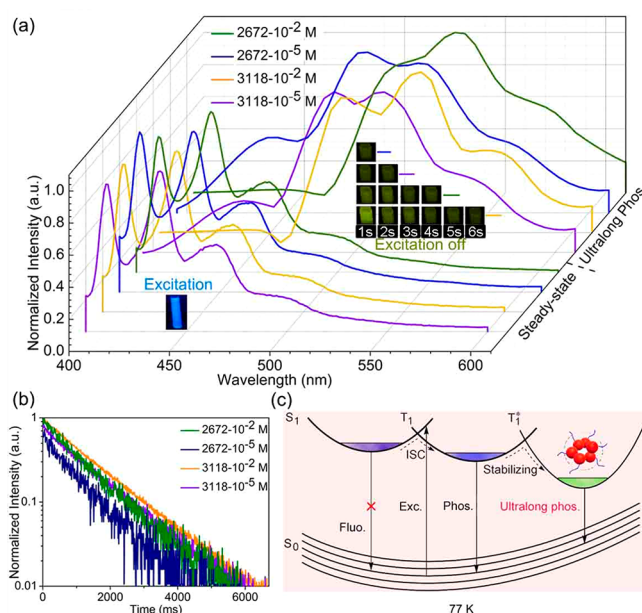


Figure 3. (a) Steady-state photoluminescence and long-phosphorescence spectra of PU1 with different average molecular weights ($M_n = 2672$ or 3118 g mol^{-1}) and different concentrations in 2-MeTHF solutions at 77 K. Insets show the corresponding photographs taken at different times before and after turning off the excitation (365 nm) at 77 K. (b) Phosphorescence decays at 560 nm of PU1 in 2-MeTHF solution. (c) Proposed LPL mechanism for PU1 at 77 K.

nonconjugated polymer.^{38–41} The resistance of the low-temperature phosphorescence to photobleaching was further confirmed by 20 repeated excitation cycles with high reproducibility (Figure S11). To further investigate this rare LPL, transition-state emission spectra (TRES) were obtained. As shown in Figure 3a, the TRES of PU1 showed multiple emission profiles with major peaks at 445, 490, 513, and 560 nm. Decay times corresponding to emission peaks were measured individually. Interestingly, in contrast to the fast fluorescent emission ($S_1 \rightarrow S_0$) with lifetimes of a few nanoseconds at room temperature, long-persistent phosphorescent (T_1) lifetimes beyond a few hundred milliseconds were observed in each peak (Table S1). The longest luminescent lifetime of 1.4 s was observed in the 560 nm peak (Figure 3b). For comparison, a lifetime of 1.2 s has been reported at room temperature for poly(methyl methacrylate) (PMMA) with an *N*-substituted naphthalimide end group.⁴² Poly(lactic acid) functionalized with difluoroboron dibenzoylmethane has a lifetime of 1.75 s at 77 K.⁴³ Thus, the T_1 excited state with long decay times dominates the emission behavior of PU1 at 77 K. It is known that at low temperature, the rates of internal conversion (IC), intersystem crossing (ISC), and collisional quenching are commonly restricted because of the rigidity of the frozen sample, resulting in phosphorescence with microsecond decay times.⁴⁴ However, to the best of our knowledge, such long-persistent phosphorescence (~ 0.8 s) has not been previously reported in an organic polymer at 77 K at a concentration as low as 10^{-5} M (Table S1).

What is the reason for this unusual LPL phenomenon? On the basis of the formation of nanoparticles at low concentration (10^{-5} M) of PU1, as observed from the TEM image (Figure S6a), we propose that the electron-rich heteroatoms and the good flexibility in the polyurethane chains promote the formation of clusters through intra- and/or intermolecular

interactions even at this low concentration. This is a different situation from pure small organic molecules that are regarded as isolated molecules without any intra- or intermolecular interactions in dilute solution.⁴⁵ The spatial electronic overlap between lone pairs and π electrons within the carbonyl clusters in PU1 explains the fascinating cryogenic long-persistent phosphorescence. To validate our hypothesis, PMMA matrices doped with PU1 (2%) were used in solid-state “dilution” experiments to probe the role of intramolecular motions in the observation of LPL. In contrast to the long phosphorescent lifetime (~ 0.8 s) observed in the low-concentration solutions of pure PU1 at 77 K, a PMMA-doped film exhibited a short fluorescent lifetime of 2 ns (Figure S12). This confirms that effectively restricting intramolecular motions is not the reason for the observed LPL of PU1 at 77 K.

More detailed photophysical measurements certify that carbonyl clusters play a key role in obtaining LPL. Concentration-dependent emission data in 2-MeTHF solution are shown in Figure 3b and Table S1. Persistent phosphorescence with λ_{max} at 560 nm was selected, and the decay time of PU1 increased from 0.76 to 1.44 s upon increasing the concentration from 10^{-5} to 10^{-2} M. This concentration-promoted LPL is consistent with the formation of clusters. Furthermore, the influence of different degrees of polymerization in PU1 on LPL was also considered by comparing samples with $M_n = 3118$ and 2672 g mol $^{-1}$. The two samples showed similar concentration-dependent LPL (Figure 3b and Table S1). It is worth noting that the decay lifetime increases significantly with the increased degree of polymerization (Figure 3b and Table S1). This can be attributed to increased formation of clusters by the more flexible chains and the electron-rich heteroatoms of PU1 (3118 g mol $^{-1}$). In contrast to the long phosphorescent lifetime (~ 0.8 s) observed for PU1 at 77 K, (R)-BINOL exhibited a short phosphorescent lifetime of 8.77 μ s in dilute 2-MeTHF solution (Figure S13). Therefore, all the above results provide substantial evidence that aggregation induced by carbonyl clusters is a key requisite for LPL at 77 K in PU1.

In the powder state of PU1, LPL is also observed for both molecular weight samples ($M_n = 3118$ and 2672 g mol $^{-1}$) at 77 K. The transition-state emission spectra of PU1 show a broad emission band with peaks at 520 and 550 nm (Figures 4a,b). LPL behavior of PU1 (3118 g mol $^{-1}$) was observed by the naked eye for a period of 4 s, and the corresponding decay time was 0.52 s. Similar to the solution state, an increased decay time was observed from the lower molecular weight (2672 g mol $^{-1}$, 0.44 s) compared to the higher molecular weight (3118 g mol $^{-1}$, 0.52 s) of powder samples of PU1 (Figure S15 and Table S2, $\lambda_{\text{max}} = 550$ nm). The lifetime data for PU1 ($M_n = 2672$ g mol $^{-1}$) in the pristine film state at two different concentrations of 10 and 100 mg were also investigated at 77 K. There is an increase in luminescence lifetime with increasing concentration of PU1 (Table S3).

To further probe the LPL mechanism of PU1, the S_1 and T_1 energy levels were estimated from the onset wavelengths of the 298 and 77 K steady-state emission spectra (Figure S16), respectively, measured in solution. The small S_1 – T_1 energy gap ($\Delta E_{\text{ST}} = 0.06$ eV) could promote the ISC as well as reverse ISC processes, thus prolonging the excited-state lifetimes.³⁴ At room temperature, fast fluorescence from the S_1 state with a lifetime of a few nanoseconds is observed because of the spin-forbidden T_1 state. Meanwhile, thermally activated delayed fluorescence (TADF) was not observed, perhaps because of a lack of spin–

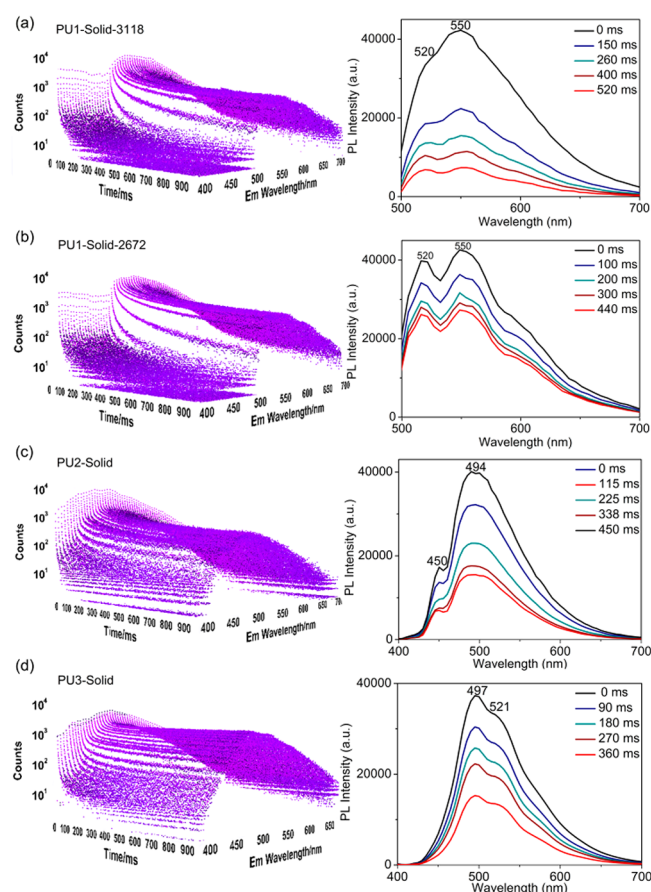


Figure 4. 3D time-resolved emission spectra (TRES) (left) and corresponding transition-state emission spectra (right) of PU1–PU3 in powder state at 77 K.

vibronic coupling.⁴⁶ At 77 K, assisted by the low temperature, the singlet excitons were rapidly converted to triplet excitons through a fast ISC process, and bright blue phosphorescence was observed in steady-state conditions; the corresponding T_1 energy level was calculated to be 3.09 eV (Figure S16). Upon removal of the ultraviolet irradiation, the emission color changed from blue to green-yellow with a lower energy level of 2.71 eV (Figure S16). This result is evidence for the existence of a stabilized excited state (T_1^*) that functions as an energy trap and may be delocalized on several neighboring polyurethane chains,⁴⁷ resulting in long phosphorescence by facilitating radiative pathways and suppressing nonradiative deactivation decays. The proposed LPL mechanism of PU1 is shown in Figure 3c.

Intermolecular n – π^* transitions from electron-rich heteroatoms to conjugated (hetero)aromatic units in small molecules have been shown by the groups of Chi,⁴⁸ Li,⁴⁹ Huang,⁵⁰ and Tang^{51–53} to facilitate ISC leading to LPL behavior. Recently, Li et al. reported that intermolecular π – π interactions play an important role in persistent phosphorescence.^{54–56} Therefore, it is rational to check the role of the aromatic unit in obtaining LPL in our polyurethane system. For comparison with PU1, analogs were prepared with a smaller biphenyl unit (PU2, $M_n = 1845$ g mol $^{-1}$) and with a saturated unit (PU3, $M_n = 3544$ g mol $^{-1}$), replacing the binaphthyl unit of PU1. The luminescence decays of PU2 and PU3 were measured in the powder state at 77 K. As shown in Figure 4c,d and Table S2, both PU2 and PU3 exhibit LPL behavior,

demonstrating that the aromatic unit is not essential for LPL in polyurethane derivatives. Nonetheless, the decay times clearly increase with the introduction of aromatic units into the nonconjugated PU chains (Table S2), revealing that the intra- or intermolecular $n-\pi^*$ transition from electron-rich carbonyl groups to the conjugated aromatic units is favorable for enhancing LPL behavior.

2.4. Cryogenic Afterglow LED. To investigate the potential optoelectronic applications of the polyurethane materials, a cryogenic afterglow LED was fabricated by adding dropwise a solution of PU1 ($M_n = 2672 \text{ g mol}^{-1}$) in 2-MeTHF onto an ultraviolet InGaAsN LED chip ($\lambda_{\text{em}} = 395 \text{ nm}$). As shown in Figure 5b, because of the favorable viscosity of the

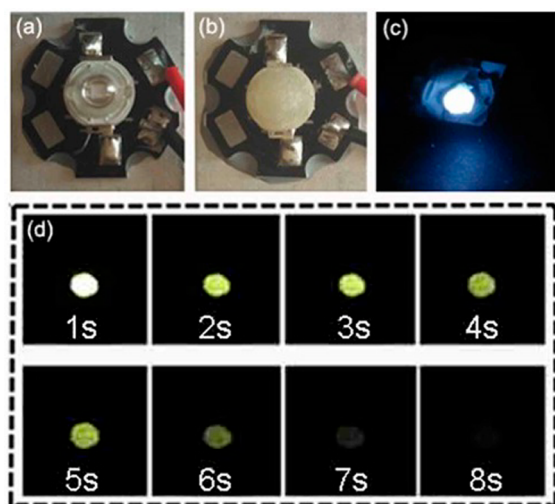


Figure 5. (a) An emitting 3 mm diameter reference ultraviolet InGaAsN LED ($\lambda_{\text{em}} = 395 \text{ nm}$). (b) The same LED coated with a thin layer of 3.5 wt % PU1 (not turned on). (c) The coated LED was turned on immediately after it was removed from liquid nitrogen and emits bright blue emission. (d) Phosphorescence images taken at 1 s intervals after turning off the operating voltage.

polymer, PU1 (50 mg) uniformly adheres to the surface of the LED to form a thin film. Immediately after the LED bulb is removed from the 77 K environment, upon electrical excitation with a low voltage (3 V), bright blue emission was obtained (Figure 5c). When the applied voltage was turned off, green persistent emission is observed for as long as 7 s, attributed to the phosphorescence of PU1 (Figure 5d and Supplementary Movie 2).

3. CONCLUSION

In summary, visible long-lived luminescence ($>1 \text{ s}$) in a nonconjugated polyurethane system at 77 K has been reported for the first time. The aggregation-induced LPL mechanism was shown by detailed photophysical and time-resolved emission spectra to arise from spatial electronic overlap between lone pairs and π electrons through the formation of carbonyl clusters. The introduction of conjugated aromatic units into the backbone of the nonconjugated polymer chains has been shown to promote the ISC process through intra- or intermolecular $n-\pi^*$ transitions and further increase the decay times of LPL. Furthermore, benefiting from the excellent aggregation-induced LPL, a cryogenic afterglow light-emitting diode (LED) has been fabricated and persistent phosphorescence has been observed for up to 7 s by naked eyes. This

work should promote new studies on the rational design of nonconjugated polymers that display aggregation-induced long-lived luminescence, leading to further applications in optoelectronic technologies. In the future, unconventional ultralong-lived luminescence may be realized by tailoring the structure of a nonconjugated polymer.

4. EXPERIMENTAL SECTION

4.1. Synthesis. PU1 was prepared according to the following general procedure: A mixture of (R)-BINOL (0.750 g, 2.62 mmol), polyethylene glycol monomethyl ether ($M_w = 200 \text{ g mol}^{-1}$; 0.396 g, 1.98 mmol), anhydrous THF (10 mL), hexam-ethylene di-isocyanate (0.608 g, 3.61 mmol), and DABCO (12 mg, 0.105 mmol) was heated at 75 °C for 7 h under a nitrogen atmosphere until the clear solution became significantly viscous, indicating polymerization. After being cooled to room temperature, the mixture was precipitated from excess diethyl ether. Then the product was dried under vacuum at room temperature for 24 h to obtain the resulting polymer. Yield: 61%. ^1H NMR (500 MHz, DMSO- d_6 , δ [ppm]): 7.01–8.08 (broad, 12H; (R)-BINOL protons), 4.04 (s, 4H), 3.37–3.58 (broad, PEG protons), 3.32 (s, 6H; PEG terminal $-\text{OCH}_3$ protons), 2.63–2.98 (broad, 4H), 1.09 (broad, 4H), 0.75 (broad, 4H). FTIR: 3339 cm^{-1} (N–H), 2860 and 2941 cm^{-1} ($-\text{CH}_2-$ asymmetric and symmetric stretch), 1692 ($\text{C}=\text{O}$), 1113 cm^{-1} ($\text{C}-\text{O}-\text{C}$ stretch PEG). Anal. Calcd for $\text{C}_{46}\text{H}_{62}\text{N}_4\text{O}_{11}$: C, 65.24; H, 7.33; N, 6.62. Found: C, 65.38; H, 7.16; N, 6.16. $M_n = 3118 \text{ g mol}^{-1}$; PDI = 1.52.

The synthetic procedure for PU2 was the same as that for PU1, except monomer 2,2'-biphenol (0.488 g, 2.62 mmol) was used instead of (R)-BINOL. Yield: 63%. ^1H NMR (500 MHz, DMSO- d_6 , δ [ppm]): 7.02–7.44 (broad, 8H; 2,2'-biphenol protons), 4.03 (s, 4H), 3.40–3.60 (broad, PEG protons), 3.32 (s, 6H; PEG terminal $-\text{OCH}_3$ protons), 2.88 (broad, 4H), 1.16 (broad, 4H), 1.32 (broad, 4H). FTIR: 3327 cm^{-1} (N–H), 2858 and 2933 cm^{-1} ($-\text{CH}_2-$ asymmetric and symmetric stretching), 1715 cm^{-1} ($\text{C}=\text{O}$), 1111 cm^{-1} ($\text{C}-\text{O}-\text{C}$ stretching PEG). Anal. Calcd for $\text{C}_{38}\text{H}_{58}\text{N}_4\text{O}_{11}$: C, 61.13; H, 7.77; N, 7.51. Found: C, 61.38; H, 7.16; N, 8.16. $M_n = 1845 \text{ g mol}^{-1}$; PDI = 1.16.

The synthetic procedure for PU3 was the same as that for PU1, except monomer 1,2-ethanediol (0.163 g, 2.62 mmol) was used instead of (R)-BINOL. Yield: 64%. ^1H NMR (500 MHz, DMSO- d_6 , δ [ppm]): 7.16 (s, 2H), 4.06 (broad, 4H), 3.93 (broad, 4H), 3.41–3.58 (broad, PEG protons), 3.32 (s, 6H; PEG terminal $-\text{OCH}_3$ protons), 2.94 (s, 4H), 1.35 (s, 4H), 1.22 (s, 4H). FTIR: 3326 cm^{-1} (N–H), 2862 and 2939 cm^{-1} ($-\text{CH}_2-$ asymmetric and symmetric stretching), 1684 cm^{-1} ($\text{C}=\text{O}$), 1144 cm^{-1} ($\text{C}-\text{O}-\text{C}$ stretching PEG). Anal. Calcd for $\text{C}_{36}\text{H}_{54}\text{N}_4\text{O}_{11}$: C, 60.17; H, 7.52; N, 7.80; O, 24.51. Found: C, 60.38; H, 7.46; N, 7.86; O, 24.30. The M_n of PU3 is 3544 g mol^{-1} calculated from the ^1H NMR spectra.

4.2. Photophysical Characterization. UV-vis absorption spectra were recorded on a Shimadzu UV-3100 spectrophotometer. Steady-state emission spectra, the excited-state lifetimes (τ), photoluminescence quantum yields (Φ_p), and time-resolved emission spectra (TRES) were recorded on an Edinburgh FLS-920 spectrofluorimeter equipped with a xenon arc lamp (Xe900), a nanosecond hydrogen flash-lamp (nF920), and a microsecond flash-lamp (μ F900), respectively. For fluorescence decay measurements, subnanosecond optical pulses over the VUV-to-NIR spectral range were provided using a hydrogen flash lamp. The microsecond flash lamp produces short, typically a few microseconds, and high-irradiance optical pulses for phosphorescence decay measurements in the range from microseconds to seconds. The lifetimes (τ) of the luminescence were obtained by fitting the decay curve with a multiexponential decay function

$$I(t) = \sum_i A_i e^{-t/\tau_i}$$

where A_i and τ_i represent the amplitudes and lifetimes, respectively, of the individual components for multiexponential decay profiles.

4.3. Fabrication of Cryogenic Afterglow LED. A cryogenic afterglow light-emitting diode (LED) was fabricated by dropwise addition of a solution of PU1 ($M_n = 2672 \text{ g mol}^{-1}$, 50 mg, 3.5 wt %) in 2-MeTHF on an ultraviolet InGaAsN LED chip ($\lambda_{\text{em}} = 395 \text{ nm}$) at room temperature. The photographs and [supplementary movies](#) were recorded with a cell phone (Huawei Nova 1).

■ ASSOCIATED CONTENT

Supporting Information

The Supporting Information is available free of charge on the ACS Publications website at DOI: [10.1021/acs.macromol.8b00715](https://doi.org/10.1021/acs.macromol.8b00715).

Additional structural characterization, copies of NMR and FTIR spectra, additional photophysical data, and TEM data ([PDF](#))

Supplementary Movie 1 (ultralong phosphorescence at 77 K) ([AVI](#))

Supplementary Movie 2 (persistent emission) ([AVI](#))

■ AUTHOR INFORMATION

Corresponding Authors

*E-mail: zhudx047@nenu.edu.cn.

*E-mail: zmsu@nenu.edu.cn.

*E-mail: m.r.bryce@durham.ac.uk.

ORCID

Bao-Hua Zhang: 0000-0002-5441-4159

Zhong-Min Su: 0000-0002-3342-1966

Martin R. Bryce: 0000-0003-2097-7823

Author Contributions

^{||}N.J. and G.-F.L. contributed equally.

Notes

The authors declare no competing financial interest.

■ ACKNOWLEDGMENTS

The work was funded by NSFC (No. 51473028), the key scientific and technological project of Jilin province (20150204011GX, 20160307016GX), and the Development and Reform Commission of Jilin province (20160058). M.R.B. acknowledges EPSRC Grant EP/L02621X/1 for funding.

■ REFERENCES

- (1) Mei, J.; Leung, N. L.; Kwok, R. T.; Lam, J. W.; Tang, B. Z. Aggregation-Induced Emission: Together We Shine, United We Soar! *Chem. Rev.* **2015**, *115*, 11718–11940.
- (2) Zhang Yuan, W.; Zhang, Y. Nonconventional macromolecular luminogens with aggregation-induced emission characteristics. *J. Polym. Sci., Part A: Polym. Chem.* **2017**, *55*, 560–574.
- (3) Restani, R. B.; Morgado, P. I.; Ribeiro, M. P.; Correia, I. J.; Aguiar-Ricardo, A.; Bonifacio, V. D. Biocompatible Polyurea Dendrimers with pH-Dependent Fluorescence. *Angew. Chem., Int. Ed.* **2012**, *51*, 5162–5165.
- (4) Sun, M.; Hong, C. Y.; Pan, C. Y. A unique aliphatic tertiary amine chromophore: fluorescence, polymer structure, and application in cell imaging. *J. Am. Chem. Soc.* **2012**, *134*, 20581–20584.
- (5) Zhu, S.; Song, Y.; Shao, J.; Zhao, X.; Yang, B. Non-Conjugated Polymer Dots with Crosslink-Enhanced Emission in the Absence of Fluorophore Units. *Angew. Chem., Int. Ed.* **2015**, *54*, 14626–14637.
- (6) Huang, T.; Wang, Z.; Qin, A.; Sun, J.; Tang, B. Luminescent polymers containing unconventional chromophores. *Huaxue Xuebao* **2013**, *71*, 979–990.
- (7) Lee, W. I.; Bae, Y.; Bard, A. J. Strong blue photoluminescence and ECL from OH-terminated PAMAM dendrimers in the absence of gold nanoparticles. *J. Am. Chem. Soc.* **2004**, *126*, 8358–8359.

(8) Wang, D. J.; Imae, T. Fluorescence emission from dendrimers and its pH dependence. *J. Am. Chem. Soc.* **2004**, *126*, 13204–13205.

(9) Wu, D. C.; Liu, Y.; He, C. B.; Goh, S. H. Blue Photoluminescence from Hyperbranched Poly(amino ester)s. *Macromolecules* **2005**, *38*, 9906–9909.

(10) Chu, C. C.; Imae, T. Fluorescence Investigations of Oxygen-Doped Simple Amine Compared with Fluorescent PAMAM Dendrimer. *Macromol. Rapid Commun.* **2009**, *30*, 89–93.

(11) Lin, S. Y.; Wu, T. H.; Jao, Y. C.; Liu, C. P.; Lin, H. Y.; Lo, L. W.; Yang, C. S. Unraveling the Photoluminescence Puzzle of PAMAM Dendrimers. *Chem. - Eur. J.* **2011**, *17*, 7158–7161.

(12) Pastor-Pérez, L.; Chen, Y.; Shen, Z.; Lahoz, A.; Stiriba, S. E. Unprecedented Blue Intrinsic Photoluminescence from Hyperbranched and Linear Polyethylenimines: Polymer Architectures and pH-Effects. *Macromol. Rapid Commun.* **2007**, *28*, 1404–1409.

(13) Wang, R. B.; Yuan, W. Z.; Zhu, X. Y. Aggregation-induced emission of non-conjugated poly(amido amine)s: discovering, luminescent mechanism understanding and bioapplication. *Chin. J. Polym. Sci.* **2015**, *33*, 680–687.

(14) Yu, W.; Wu, Y.; Chen, J.; Duan, X.; Jiang, X. F.; Qiu, X.; Li, Y. Sulfonated ethylenediamine–acetone–formaldehyde condensate: preparation, unconventional photoluminescence and aggregation enhanced emission. *RSC Adv.* **2016**, *6*, 51257–51263.

(15) Gong, Y.; Tan, Y.; Mei, J.; Zhang, Y.; Yuan, W.; Zhang, Y.; Sun, J.; Tang, B. Z. Room temperature phosphorescence from natural products: Crystallization matters. *Sci. China: Chem.* **2013**, *56*, 1178–1182.

(16) Niu, S.; Yan, H.; Chen, Z.; Yuan, L.; Liu, T.; Liu, C. Water-Soluble Blue Fluorescence-Emitting Hyperbranched Polysiloxanes Simultaneously Containing Hydroxyl and Primary Amine Groups. *Macromol. Rapid Commun.* **2016**, *37*, 136–142.

(17) Pucci, A.; Rausa, R.; Ciardelli, F. Aggregation-Induced Luminescence of Polyisobutene Succinic Anhydrides and Imides. *Macromol. Chem. Phys.* **2008**, *209*, 900–906.

(18) Yu, W.; Wang, Z.; Yang, D.; Ouyang, X.; Qiu, X.; Li, Y. Nonconventional photoluminescence from sulfonated acetone–formaldehyde condensate with aggregation-enhanced emission. *RSC Adv.* **2016**, *6*, 47632–47636.

(19) Zhao, E.; Lam, J. W. Y.; Meng, L.; Hong, Y.; Deng, H.; Bai, G.; Huang, X.; Hao, J.; Tang, B. Z. Poly[(maleic anhydride)-*alt*-(vinyl acetate)]: A Pure Oxygenic Nonconjugated Macromolecule with Strong Light Emission and Solvatochromic Effect. *Macromolecules* **2015**, *48*, 64–71.

(20) Bhattacharya, S.; Rao, V. N.; Sarkar, S.; Shunmugam, R. Unusual emission from norbornene derived phosphonate molecule—a sensor for Fe^{III} in aqueous environment. *Nanoscale* **2012**, *4*, 6962–6966.

(21) Liu, T.; Meng, Y.; Wang, X.; Wang, H.; Li, X. Unusual strong fluorescence of a hyperbranched phosphate: discovery and explanations. *RSC Adv.* **2013**, *3*, 8269–8275.

(22) Li, W.; Wu, X.; Zhao, Z.; Qin, A.; Hu, R.; Tang, B. Z. Catalyst-free, atom-economic, multicomponent polymerizations of aromatic diynes, elemental sulfur, and aliphatic diamines toward luminescent polythioamides. *Macromolecules* **2015**, *48*, 7747–7754.

(23) Yan, J.; Zheng, B.; Pan, D.; Yang, R.; Xu, Y.; Wang, L.; Yang, M. Unexpected fluorescence from polymers containing dithio/amino-succinimides. *Polym. Chem.* **2015**, *6*, 6133–6139.

(24) Lu, H.; Feng, L.; Li, S.; Zhang, J.; Lu, H.; Feng, S. Unexpected Strong Blue Photoluminescence Produced from the Aggregation of Unconventional Chromophores in Novel Siloxane–Poly-(amidoamine) Dendrimers. *Macromolecules* **2015**, *48*, 476–482.

(25) Yang, L.; Wang, L.; Cui, C.; Lei, J.; Zhang, J. Stöber strategy for synthesizing multifluorescent organosilica nanocrystals. *Chem. Commun.* **2016**, *52*, 6154–6157.

(26) Zhou, Q.; Cao, B.; Zhu, C.; Xu, S.; Gong, Y.; Yuan, W. Z.; Zhang, Y. Clustering-Triggered Emission of Nonconjugated Polyacrylonitrile. *Small* **2016**, *12*, 6586–6592.

(27) Lendlein, A.; Kelch, S. Shape-memory polymers. *Angew. Chem., Int. Ed.* **2002**, *41*, 2034–2057.

- (28) Chattopadhyay, D. K.; Raju, K. V. S. N. Structural engineering of polyurethane coatings for high performance applications. *Prog. Polym. Sci.* **2007**, *32*, 352–418.
- (29) Liu, C.; Qin, H.; Mather, P. T. Review of progress in shape-memory polymers. *J. Mater. Chem.* **2007**, *17*, 1543–1558.
- (30) Fan, Z. X.; Zhao, Q. H.; Wang, S.; Bai, Y.; Wang, P. P.; Li, J. J.; Chu, Z. W.; Chen, G. H. Polyurethane foam functionalized with an AIE-active polymer using an ultrasonication-assisted method: preparation and application for the detection of explosives. *RSC Adv.* **2016**, *6*, 26950–26953.
- (31) Niu, Y. Q.; He, T.; Song, J.; Chen, S. P.; Liu, X. Y.; Chen, Z. G.; Yu, Y. J.; Chen, S. G. A new AIE multi-block polyurethane copolymer material for subcellular microfilament imaging in living cells. *Chem. Commun.* **2017**, *53*, 7541–7544.
- (32) Wu, Y.; Hu, J.; Huang, H.; Li, J.; Zhu, Y.; Tang, B.; Han, J.; Li, L. Memory chromic polyurethane with tetraphenylethylene. *J. Polym. Sci., Part B: Polym. Phys.* **2014**, *52*, 104–110.
- (33) Sun, W.; Wang, Z.; Wang, T.; Yang, L.; Jiang, J.; Zhang, X.; Luo, Y.; Zhang, G. Protonation-Induced Room-Temperature Phosphorescence in Fluorescent Polyurethane. *J. Phys. Chem. A* **2017**, *121*, 4225–4232.
- (34) Dias, F. B.; Bourdakos, K. N.; Jankus, V.; Moss, K. C.; Kamtekar, K. T.; Bhalla, V.; Santos, J.; Bryce, M. R.; Monkman, A. P. Triplet harvesting with 100% efficiency by way of thermally activated delayed fluorescence in charge transfer OLED emitters. *Adv. Mater.* **2013**, *25*, 3707–3714.
- (35) Mei, J.; Hong, Y.; Lam, J. W.; Qin, A.; Tang, Y.; Tang, B. Z. Aggregation-induced emission: the whole is more brilliant than the parts. *Adv. Mater.* **2014**, *26*, 5429–5479.
- (36) Wan, Q.; Liu, M.; Mao, L.; Jiang, R.; Xu, D.; Huang, H.; Dai, Y.; Deng, F.; Zhang, X.; Wei, Y. Preparation of PEGylated polymeric nanoprobes with aggregation-induced emission feature through the combination of chain transfer free radical polymerization and multicomponent reaction: Self-assembly, characterization and biological imaging applications. *Mater. Sci. Eng., C* **2017**, *72*, 352–358.
- (37) Mohamed, M. G.; Lu, F.-H.; Hong, J.-L.; Kuo, S.-W. Strong emission of 2,4,6-triphenylpyridine-functionalized polytyrosine and hydrogen-bonding interactions with poly (4-vinylpyridine). *Polym. Chem.* **2015**, *6*, 6340–6350.
- (38) Zhang, G.; Chen, J.; Payne, S. J.; Kooi, S. E.; Demas, J. N.; Fraser, C. L. Multi-emissive difluoroboron dibenzoylmethane polylactide exhibiting intense fluorescence and oxygen-sensitive room-temperature phosphorescence. *J. Am. Chem. Soc.* **2007**, *129*, 8942–8943.
- (39) Zhang, G.; Palmer, G. M.; Dewhirst, M. W.; Fraser, C. L. A dual-emissive-materials design concept enables tumour hypoxia imaging. *Nat. Mater.* **2009**, *8*, 747–751.
- (40) Zhang, X.; Xie, T.; Cui, M.; Yang, L.; Sun, X.; Jiang, J.; Zhang, G. General design strategy for aromatic ketone-based single component dual-emissive materials. *ACS Appl. Mater. Interfaces* **2014**, *6*, 2279–2284.
- (41) Zhou, C.; Xie, T.; Zhou, R.; Trindle, C. O.; Tikman, Y.; Zhang, X.; Zhang, G. Waterborne polyurethanes with tunable fluorescence and room temperature phosphorescence. *ACS Appl. Mater. Interfaces* **2015**, *7*, 17209–17216.
- (42) Chen, X.; Xu, C.; Wang, T.; Zhou, C.; Du, J.; Wang, Z.; Xu, H.; Xie, T.; Bi, G.; Jiang, J.; Zhang, X.; Demas, J. N.; Trindle, C. O.; Luo, Y.; Zhang, G. Versatile room-temperature-phosphorescent materials prepared from N-substituted naphthalimides: emission enhancement and chemical conjugation. *Angew. Chem., Int. Ed.* **2016**, *55*, 9872–9876.
- (43) Zhang, G.; Evans, R. E.; Campbell, K. A.; Fraser, C. L. Role of boron in the polymer chemistry and photophysical properties of difluoroboron–dibenzoylmethane polylactide. *Macromolecules* **2009**, *42*, 8627–8633.
- (44) Menning, S.; Kramer, M.; Coombs, B. A.; Rominger, F.; Beeby, A.; Dreuw, A.; Bunz, U. H. Twisted tethered tolans: Unanticipated long-lived phosphorescence at 77 K. *J. Am. Chem. Soc.* **2013**, *135*, 2160–2163.
- (45) Hong, Y.; Lam, J. W. Y.; Tang, B. Z. Aggregation-induced emission: phenomenon, mechanism and applications. *Chem. Commun.* **2009**, 4332–4353.
- (46) Etherington, M. K.; Gibson, J.; Higginbotham, H. F.; Penfold, T. J.; Monkman, A. P. Revealing the spin–vibronic coupling mechanism of thermally activated delayed fluorescence. *Nat. Commun.* **2016**, *7*, 13680.
- (47) Congreve, D. N.; Lee, J.; Thompson, N. J.; Hontz, E.; Yost, S. R.; Reuswig, P. D.; Bahlke, M. E.; Reineke, S.; Van Voorhis, T.; Baldo, M. A. External quantum efficiency above 100% in a singlet-exciton-fission–based organic photovoltaic cell. *Science* **2013**, *340*, 334–337.
- (48) Yang, Z.; Mao, Z.; Zhang, X.; Ou, D.; Mu, Y.; Zhang, Y.; Zhao, C.; Liu, S.; Chi, Z.; Xu, J.; Wu, Y. C.; Lu, P. Y.; Lien, A.; Bryce, M. R. Intermolecular Electronic Coupling of Organic Units for Efficient Persistent Room-Temperature Phosphorescence. *Angew. Chem., Int. Ed.* **2016**, *55*, 2181–2185.
- (49) Xie, Y.; Ge, Y.; Peng, Q.; Li, C.; Li, Q.; Li, Z. How the Molecular Packing Affects the Room Temperature Phosphorescence in Pure Organic Compounds: Ingenious Molecular Design, Detailed Crystal Analysis, and Rational Theoretical Calculations. *Adv. Mater.* **2017**, *29*, 1606829.
- (50) An, Z.; Zheng, C.; Tao, Y.; Chen, R.; Shi, H.; Chen, T.; Wang, Z.; Li, H.; Deng, R.; Liu, X.; Huang, W. Stabilizing triplet excited states for ultralong organic phosphorescence. *Nat. Mater.* **2015**, *14*, 685–690.
- (51) He, Z.; Zhao, W.; Lam, J. W. Y.; Peng, Q.; Ma, H.; Liang, G.; Shuai, Z.; Tang, B. Z. White light emission from a single organic molecule with dual phosphorescence at room temperature. *Nat. Commun.* **2017**, *8*, 416.
- (52) Yuan, W. Z.; Shen, X. Y.; Zhao, H.; Lam, J. W. Y.; Tang, L.; Lu, P.; Wang, C.; Liu, Y.; Wang, Z.; Zheng, Q.; Sun, J. Z.; Ma, Y.; Tang, B. Z. Crystallization-induced phosphorescence of pure organic luminogens at room temperature. *J. Phys. Chem. C* **2010**, *114*, 6090–6099.
- (53) Zhao, W.; He, Z.; Lam, J. W. Y.; Peng, Q.; Ma, H.; Shuai, Z.; Bai, G.; Hao, J.; Tang, B. Z. Rational molecular design for achieving persistent and efficient pure organic room-temperature phosphorescence. *Chem.* **2016**, *1*, 592–602.
- (54) Li, Q.; Li, Z. The strong light-emission materials in the aggregated state: what happens from a single molecule to the collective group. *Adv. Sci.* **2017**, *4*, 1600484.
- (55) Yang, J.; Ren, Z.; Xie, Z.; Liu, Y.; Wang, C.; Xie, Y.; Peng, Q.; Xu, B.; Tian, W.; Zhang, F.; Chi, Z.; Li, Q.; Li, Z. AIEgen with fluorescence–phosphorescence dual mechanoluminescence at room temperature. *Angew. Chem., Int. Ed.* **2017**, *56*, 880–884.
- (56) Yang, J.; Zhen, X.; Wang, B.; Gao, X.; Ren, Z.; Wang, J.; Xie, Y.; Li, J.; Peng, Q.; Pu, K.; Li, Z. The influence of the molecular packing on the room temperature phosphorescence of purely organic luminogens. *Nat. Commun.* **2018**, *9*, 840.